Review

Topographic Variation of the Growth Rate of Geographic Atrophy in Nonexudative Age-Related Macular Degeneration: A Systematic Review and Meta-analysis

Liangbo L. Shen,[1] Mengyuan Sun,[2] Sumun Khetpal,[1] Holly K. Grossetta Nardini,[3] and Lucian V. Del Priore[1]

[1]Department of Ophthalmology and Visual Science, Yale University School of Medicine, New Haven, Connecticut, United States
[2]Department of Molecular Biophysics and Biochemistry, Yale University, New Haven, Connecticut, United States
[3]Harvey Cushing/John Hay Whitney Medical Library, Yale University, New Haven, Connecticut, United States

Correspondence: Lucian V. Del Priore, Department of Ophthalmology and Visual Science, Yale University School of Medicine, 40 Temple Street, Suite 1B, New Haven, CT 06510, USA; lucian.delpriore@yale.edu.

Received: July 3, 2019
Accepted: November 10, 2019
Published: January 29, 2020

Citation: Shen LL, Sun M, Khetpal S, Grossetta Nardini HK, Del Priore LV. Topographic variation of the growth rate of geographic atrophy in nonexudative age-related macular degeneration: a systematic review and meta-analysis. *Invest Ophthalmol Vis Sci.* 2020;61(1):2. https://doi.org/10.1167/iovs.61.1.2

Purpose. To determine the impact of topographic locations on the progression rate of geographic atrophy (GA).

Methods. We searched in five literature databases up to May 3, 2019, for studies that evaluated the growth rates of GA lesions at different retinal regions. We performed random-effects meta-analyses to determine and compare the GA effective radius growth rates in four location groups defined by two separate classification schemes: (1) macular center point involved (CPI) or spared (CPS) in classification 1, and (2) foveal zone involved (FZI) or spared (FZS) in classification 2. We then estimated the GA growth rate in eight topographic zones and used the data to model the GA expansion.

Results. We included 11 studies with 3254 unique eyes. In studies that used classification 1, the effective radius growth rate was 30.1% higher in the CPS group (0.203 ± 0.013 mm/year) than in the CPI group (0.156 ± 0.011 mm/year) ($P < 0.001$). This trend became significantly more prominent in classification 2, where the growth rate was 61.7% higher in the FZS group (0.215 ± 0.012 mm/year) than in the FZI group (0.133 ± 0.009 mm/year) ($P < 0.001$). The estimated GA effective radius growth rates in eight retinal zones fit a Gaussian function, and the modeling of GA expansion gave rise to various GA configurations comparable to clinical observations.

Conclusions. This study indicates that the GA progression rate varies significantly across different retinal locations. Our analysis may shed light on the natural history and underlying mechanism of GA progression.

Keywords: age-related macular degeneration, geographic atrophy, meta-analysis, systematic review

Geographic atrophy (GA) secondary to nonexudative age-related macular degeneration (AMD) is characterized by the presence of well-demarcated borders of atrophic areas in the macula with the loss of the retinal pigment epithelium (RPE), photoreceptors, and underlying choriocapillaris.[1] GA has been reported to affect roughly 6 million people globally, and its prevalence increases dramatically with age.[2,3] During the early stage of GA, the lesion typically starts in the parafovea and then enlarges to form a ring surrounding the fovea.[4] During this stage of foveal sparing,[5–8] patients usually have decent central foveal function with preserved visual acuity.[4,9] As GA continues to progress, it will reach the fovea and result in a dramatic loss in central visual acuity and eventually legal blindness.[1,4,5,9]

Several authors have suggested that the location of GA lesions is associated with the GA progression rate.[4,10–15] Thus, it can potentially serve as a biomarker to predict the GA growth rate in patients and allow stratification for confounding in clinical trials. However, the terminologies used to describe GA locations were inconsistent in the literature, and there are at least five different terminologies: foveal or extrafoveal,[13,15,16] center involved or not involved,[10] central or noncentral,[12] subfoveal or nonsubfoveal,[11] with or without RPE atrophy under the foveal center.[14] After closely examining the definitions of the terminologies, we have found two different classification schemes to describe the baseline location of GA based on whether GA lesions involve (1) the center point of the macula (classification 1) or (2) the foveal zone (classification 2). However, even within one classification, the GA area growth rate of each group still varies widely. For example, the growth rate in GA involving the center point of the macula ranges from 1.06 to 1.89 mm^2/year.[11,12] Also, it is currently unknown which classification scheme would result in a more clinically significant difference in the GA growth rate between groups.

One likely explanation for the observed association between the location and growth rate of GA lesions is that the GA growth rate varies across different topographic

Investigative Ophthalmology & Visual Science

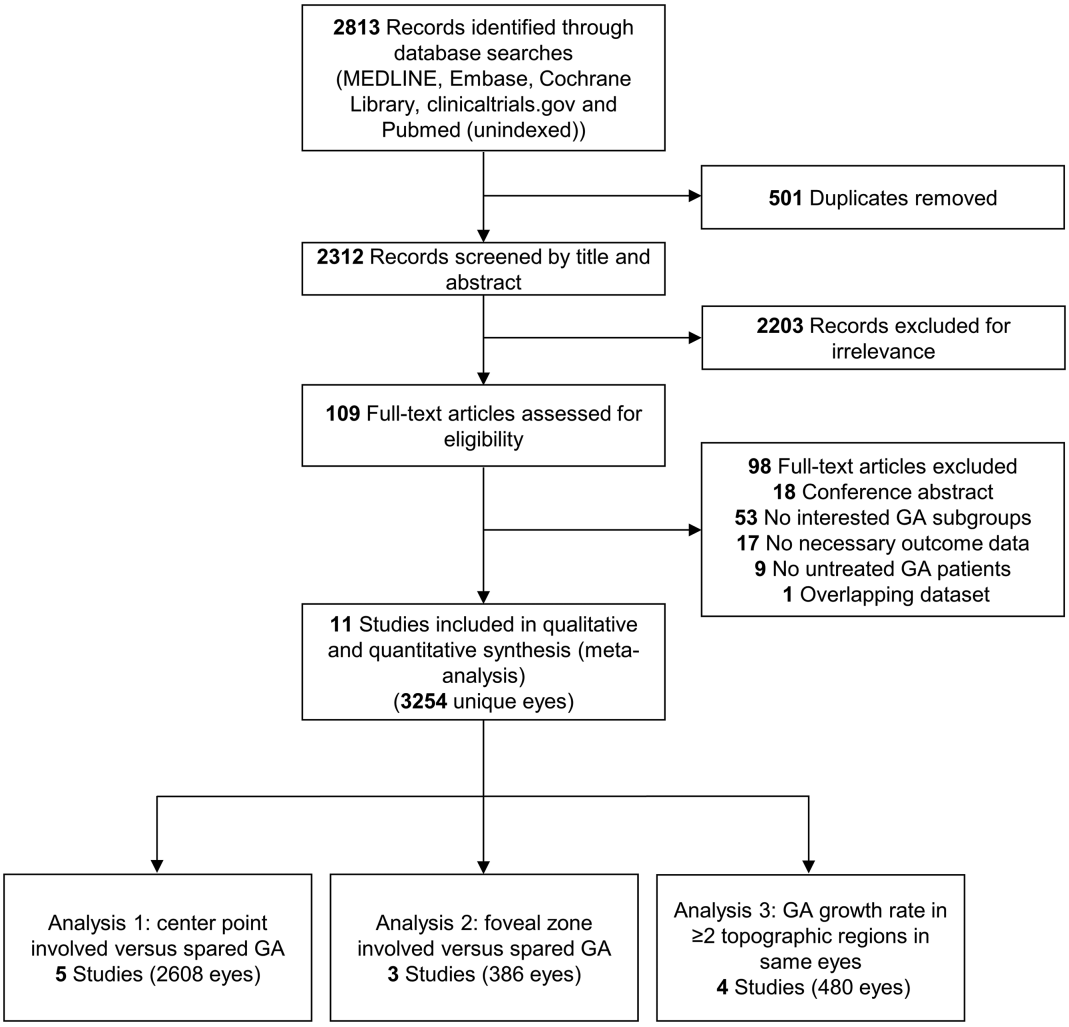

Figure 1. Preferred Reporting Items for Systematic Reviews and Meta-Analyses flowchart of identification and screening of studies. Note that one study (the geographic atrophy progression study) reported data for both analyses 1 and 3.

zones in the retina. To date, only a limited number of studies have assessed the GA progression rates in different topographic zones (usually defined as circular zones with different distances from the foveal center). Most of the prior studies have reported that GA progresses faster in the extrafovea than in the fovea.[4,9,17] However, there is a significant disagreement on the degree to which the topographic zone will impact the GA growth rate. The reported average growth rate of GA area varies dramatically in each topographic zone (e.g., 0.04–1.14 mm^2/year in the most central zone of the macula) and the definition of the topographic zones also varies among different studies.[4,9,17] Moreover, it is currently unknown whether the progression rate of GA remains constant within one topographic region or changes continuously as a function of the distance to the foveal center. The mechanism underlying the differential GA progression rates between in the fovea and extrafovea is also unclear.

To address the inconsistency in clinical data, we performed a meta-analysis to determine the GA growth rates of four groups in the two previously defined classifications. Then, we compared the two classifications to determine the one with more clinical significance. Finally, we estimated the GA effective radius growth rates in eight topographic zones in the retina. With the derived topographic profile of the GA growth rate, we modeled the expansion course of GA lesions in the retina over 30 years.

Methods

This meta-analysis is reported in accordance with the Meta-analysis Of Observational Studies in Epidemiology checklist (Supplementary Table S1).[18]

Sources and Search Methods

A senior medical librarian (H.K.G.N.) performed a comprehensive search of multiple databases for relevant studies—MEDLINE, EMBASE, Cochrane Library (Wiley), Clinicaltrials.gov, and NLM PubMed—from the start dates of the databases. All searches were updated to May 3, 2019. We did not restrict the study type, language, or published date. The search strategy is detailed in Supplementary Method. A flowchart per the Preferred Reporting Items for Systematic Reviews and Meta-Analyses is shown in Figure 1.

Investigative Ophthalmology & Visual Science

Selection Criteria

The inclusion criteria for our meta-analysis were studies that (1) included patients diagnosed with GA secondary to non-exudative AMD in at least one eye without any treatment intended to slow or halt atrophy progression; (2) photographically measured and reported GA lesion sizes on at least two occasions with a minimum of 6 months apart; and (3) evaluated growth rates of GA lesions in at least two different topographic regions in the retina.

Two types of studies met the above inclusion criteria and were included. The first type of included studies classified GA lesions based on the involvement of a retinal region and reported the growth rates of the entire GA lesions. For this type of studies, there were two classification schemes. The first scheme (classification 1) classified GA lesions based on the involvement of the center point of the macula, and we named the two location groups center point involved (CPI) and center point spared (CPS). The second scheme (classification 2) classified GA lesions based on the involvement of the foveal zone, and we named the two location groups foveal zone involved (FZI) and foveal zone spared (FZS). The second type of included studies divided the retina into different topographic zones (usually defined by circles with different radii centered at the foveal center) and reported the GA growth rates in each zone of the same eyes. For publications with an overlapping patient population, we selected the articles with the largest and most recent dataset. For interventional studies that investigated GA progression in both control and treatment (designed to slow or halt atrophy progression) groups, we included only that patient population in the control/sham group. We did not exclude patients taking oral vitamins and minerals supplements from the analysis because previous reports have shown that the supplements do not affect the GA progression rate,[12,19] and patients with advanced AMD in one eye are sometimes advised to take the supplements.[20]

Data Collection

Each record found in the literature search was screened by two of four reviewers (L.L.S., M.S, F.L., and S.K.), and we resolved disagreements through discussions. For each included study, two reviewers (L.L.S. and M.S.) independently extracted the data regarding (1) study quality; (2) demographic characteristics of the study population; (3) the mean and standard error (SE) of the total GA size (in area and effective radius) and growth rates (in area and effective radius growth rate per year); and (4) the GA area and growth rate in different topographic regions, if available. The standard error is used throughout the manuscript unless otherwise specified. Although the data regarding GA sizes at follow-ups are presented explicitly in some papers, extrapolation was necessary for other studies. For example, for studies that did not report GA effective radius or effective radius growth rate, the following estimations were made. The mean GA effective radius was calculated by $\frac{1}{\sqrt{\pi}} \times \sqrt{mean\ GA\ area}$. The mean GA effective radius growth rate was calculated by $\frac{1}{\sqrt{\pi}\times n} \times (\sqrt{A+n\times G}-\sqrt{A})$, where n is the mean follow-up time (years), A is the mean baseline area, and G is reported mean annual GA area growth rate. The SE of the GA effective radius growth rate was calculated by $\sqrt{\frac{0.0795AG_1^2n^2+0.0795A_1^2(\sqrt{A+Gn}-\sqrt{A})^2}{An^2(A+Gn)}}$, where n is mean follow-up time (years); A and A_1 are the mean and SE of baseline GA area, respectively; and G and G_1 are the mean and SE of the reported annual GA area growth rate, respectively. This equation was derived from error propagations of the function $mean\ GA\ radius\ growth\ rate = \frac{1}{\sqrt{\pi}\times n} \times (\sqrt{A+n\times G}-\sqrt{A})$. Other necessary extrapolation methods are detailed in Table 1. Disparities between the reviewers were resolved through discussion and subsequent consensus.

Data Synthesis and Statistical Analysis

The primary outcome measure in our study is the GA effective radius growth rate expressed in mm/year. This was used because our prior meta-analysis demonstrated that the effective radius of a GA lesion increases linearly as a function of time in GA lesions with sizes ranging from 2.5 to 20.3 mm^2.[21] In addition, several previous studies showed that using the square-root transformed GA area (equivalent to effective radius) reduces the dependence of the GA growth rate on the baseline.[22,23] We also reported the conventional outcome measure (GA area growth rate expressed in mm^2/year) in the present paper.

To determine and compare the GA growth rate among different GA location groups (CPI, CPS, FZI, and FZS in Table 1), we performed random-effects meta-analyses using RevMan 5.3 software (The Cochrane Collaboration, London, UK) and the metafor Meta-Analysis Package[24] for R 3.5.1 (R Foundation for Statistical Computing, Vienna, Austria). We chose the random-effects approach to allow for unexplained heterogeneity across studies.[25] To compare the mean difference in the GA growth rate (derived from the above random-effects meta-analysis) between classification 1 and classification 2, we performed an unpaired t-test. To confirm the observation that GA effective radius enlarges linearly as a function of time in each GA group, we plotted the average GA effective radius as a function of time after enrollment for each group. However, the baseline GA sizes usually vary widely among different studies,[21] suggesting that the different patient populations were at different time points of the disease course when they were enrolled in the studies. To correct for the differences in the entry time into the clinical studies, we added a horizontal translation factor (in years) to each raw data subset.[21,26–31] The translation factor essentially converted the horizontal axis from time after enrollment to inferred duration of GA, where the inferred duration of GA = time after enrollment + translation factor. To find the optimum translation factors, we first estimated a wide range for the translation factor of each study. We then adjusted one of the translation factors by 1 month at a time within the estimated range until the r^2 was maximized for the cumulative trend line with a predetermined slope of GA effective radius growth rate calculated from the above random-effects meta-analysis.

To investigate the GA growth rates in different topographic zones in the retina, we analyzed the data from studies that reported GA area distributions in at least two topographic zones in the same eye at each follow-up. Although all of these studies divided the retina into several circular zones centered at the foveal center, different studies utilized different cut-off radii for the topographic zones (Table 2). Thus, we extrapolated eight circular topographic zones using all the cut-off radii (in the distance from the foveal center) in the included studies (Supplementary

Table 1. Included Studies That Classified GA Based on Lesion Locations

Study	Study Type	Imaging Method	Mean Age (y)	No. of Eyes Included in Analysis	Length of Follow-Up (mo)	Reported Definition of GA Location Classification	Baseline GA Area (mm^2)	GA Radius Growth Rate (mm/y)	Horizontal Shift (y)
Studies with GA progression data for center point involved and center point spared GA									
Domalpally et al. (2013)[10] AREDS NCT00000145	Prospective interventional	CFP	69.7	477	48	Based on whether GA involves the center of the macula	CPI: 3.07 ± 0.25[*] CPS: 3.30 ± 0.29[*]	CPI: 0.152 ± 0.010 CPS: 0.186 ± 0.011	CPI: 6.3 CPS: 4.9
Holz et al. (2018)[11] Chroma NCT02247479	Prospective interventional	FAF	78.5	274[‖]	11	Based on whether GA involves the foveal center point	CPI: 7.95 ± 0.33[†] CPS: 7.95 ± 0.34[†]	CPI: 0.180 ± 0.009 CPS: 0.237 ± 0.010	CPI: 10.3 CPS: 7.9
Holz et al. (2018)[11] Spectri NCT02247531	Prospective interventional	FAF	77.6	291[‖]	11	Based on whether GA involves the foveal center point	CPI: 7.55 ± 0.31[†] CPS: 7.55 ± 0.36[†]	CPI: 0.179 ± 0.007 CPS: 0.232 ± 0.010	CPI: 10.0 CPS: 7.7
Keenan et al. (2018)[12] AREDS2 NCT00345176	Prospective interventional	CFP	74.9	1219	54	Based on whether GA involves the central subfield with at least questionable involvement of the center of the macula	CPI: 5.29 ± 0.16[‡] CPS: 4.49 ± 0.11[‡]	CPI: 0.124 ± 0.006 CPS: 0.175 ± 0.004	CPI: 7.9 CPS: 5.6
Rosenfeld et al. (2019)[14] SEATTLE NCT01802866	Prospective interventional	FAF	77.1	347	24	Based on whether there is RPE atrophy present under the foveal center by SD-OCT	CPI: 7.27 ± 0.27[‡] CPS: 8.04 ± 0.34[‡]	CPI: 0.147 ± 0.006 CPS: 0.186 ± 0.009	CPI: 9.7 CPS: 7.8
Studies with GA progression data for foveal zone involved and foveal zone spared GA									
Allingham et al. (2016)[16,§]	Retrospective observational	FAF	79.1	38	15.6	Not reported	FZI: 8.79 ± 1.01 FZS: 7.69 ± 2.13	FZI: 0.120 ± 0.024 FZS: 0.171 ± 0.063	FZI: 12.5 FZS: 7.1
Monés et al. (2018)[15] GAIN NCT01694095	Prospective observational	FAF	78.1	128	37.2	Not reported	FZI: 8.09 ± 0.91 FZS: 6.87 ± 0.75	FZI: 0.136 ± 0.010 FZS: 0.224 ± 0.015	FZI: 12.0 FZS: 6.8
Schmitz-Valckenberg et al. (2016)[13] GAP NCT00599846	Prospective observational	FAF	76.9	220	12	Based on whether there is atrophy involvement within a circle of 300 μm in diameter centered on the fovea	FZI: 7.00 ± 0.68[†] FZS: 7.00 ± 0.43[†]	FZI: 0.131 ± 0.020 FZS: 0.204 ± 0.020	FZI: 11.2 FZS: 6.9

GA growth rate is reported as mean ± standard error.

AREDS, age-related eye disease study; CFP, color fundus photography; FAF, fundus autofluorescence; FAM, fundus autofluorescence in age-related macular degeneration; GAIN, geographic atrophy progression in patients with age-related macular degeneration; GAP, geographic atrophy progression; SD-OCT, spectral domain optical coherence tomography; SEATTLE, safety and efficacy assessment treatment trials of emixustat hydrochloride.

[*] The mean baseline GA area is calculated as the weighted mean of baseline GA area in three individual subgroups reported in the study.

[†] For papers that did not report the mean baseline GA size in each GA location group (Holz et al., 2018; Schmitz-Valckenberg et al., 2016), we used the mean baseline GA area of the entire cohort in the corresponding study.

[‡] The mean baseline GA area was calculated from the reported annual growth rate of GA area and square root of GA area.

[§] Individual-level data were obtained from the authors in the study.

[‖] Only data from the sham-controlled arm were included.

Table 2. Studies That Investigated GA Growth Rate in at Least Two Zones in Same Eyes

Study	Study Type	Imaging Method	Mean Age (y)	No. of Eyes Included in Analysis	Length of Follow-Up (mo)	Definition of Zones in Distance from the Foveal Center (μm)	GA Area Growth Rate (mm^2/y)	GA Effective Radius Growth Rate, (mm/y[†])
Lindner et al. (2015)[38] FAM NCT00393692	Prospective observational	FAF	73.8	47	25	Residual foveal island[*]:	0.25 ± 0.03	0.065 ± 0.008
						Outside foveal island[*]:	2.27 ± 0.22	0.180 ± 0.014
Mauschitz et al. (2012)[17] GAP NCT00599846	Prospective observational	FAF	77	316	12	0–600:	0.04 ± 0.01	0.012 ± 0.002
						600–1800:	0.67 ± 0.04	0.091 ± 0.005
						1800–3600:	0.42 ± 0.05	0.133 ± 0.016
						>3600:	0.01 ± 0.01	0.008 ± 0.007
Sayegh et al. (2017)[9]	Prospective observational	OCT	76	36	18	0–500:	0.11 ± 0.04	0.052 ± 0.017
						500–1500:	0.59 ± 0.29	0.087 ± 0.041
						1500–3000:	0.73 ± 1.00	0.115 ± 0.147
Sunness et al. (1999)[5]	Prospective observational	CFP	78	81	24	0–1800:	1.14 ± 0.09	0.133 ± 0.010
						>1800:	1.14 ± 0.30	0.170 ± 0.041

GA growth rate is reported as mean ± standard error.
OCT, optical coherence tomography.
[*] Distance from the foveal center was not specified in the study.
[†] The mean GA effective radius growth rate was calculated by $\frac{1}{\sqrt{\pi}\times n} \times (\sqrt{A + n \times G} - \sqrt{A})$, where n is the mean follow-up time (y), A is the mean baseline GA area in the topographic zone, and G is the reported mean annual GA area growth rate in the topographic zone.

Table S4). Because the exact definition of the residual foveal island was not specified in Lindner et al.,[4] we used the reported average radius of the fovea (750 µm) as the cut-off radius for this zone.[32] For each extrapolated topographic zone, we then estimated the GA effective radius growth rate by calculating the weighted mean (weighted by the number of eyes in each study) of the GA effective radius growth rates in the corresponding zones from the included studies. This estimation assumes that the GA effective radius growth rate is relatively unchanged within each zone. For example, to estimate the GA effective radius growth rate in the first zone (0–500 µm from the foveal center), we calculated the weighted mean of the GA effective radius growth rates in the residual foveal island zone in Lindner et al.,[4] in the 0 to 600 µm zone in Mauschitz et al.,[17] in the 0 to 500 µm zone in Sayegh et al.,[9] and in the 0 to 1800 µm zone in Sunness et al.[5] (Supplementary Table S4). Based on the relationship between the GA effective radius growth rate and the distance to the foveal center (retinal eccentricity), we modeled the expansion course of GA lesions over 30 years using MATLAB software (MathWorks; Natick, MA). For the modeling, we used the GA effective radius growth rate (mm/year) at each location as the estimated length (mm) that the GA border would travel in 1 year at the same location.

Two reviewers (L.L.S. and M.S.) assessed the risk of bias and quality of each study using the Newcastle-Ottawa Scale,[33] which is one of the most widely used risk of bias assessment tools for meta-analysis of observational studies.[34] Inconsistencies were discussed until agreement was reached. Heterogeneity was assessed by calculating the I^2 statistic in each random-effects meta-analysis. Also, for random-effect meta-analyses with data from at least three studies, a sensitivity analysis was performed by removing one study at a time to assess whether a single study influenced the outcomes of the meta-analyses. To investigate the impact of potential confounding factors on estimated GA growth rates and statistical comparisons, we performed subgroup analysis stratified by imaging methods and study types if there were at least two studies in the subgroup.

Results

Overall Characteristics and Quality of Included Studies

The final search retrieved a total of 2312 records published before May 3, 2019, after de-duplication. After the review of the titles and abstracts, 2203 records were excluded for irrelevance. We then reviewed the full text of the remaining 109 articles and identified 11 articles from 11 studies (including 3254 unique eyes) meeting our inclusion criteria (Fig. 1).[4,5,9–17] Of note, one of the included articles (Holz et al., 2018[11]) reported data from two studies, and two of the included articles (Schmitz-Valckenberg et al., 2016[13] and Mauschitz et al., 2012[17]) were about the same study but reported data in different analyses (Tables 1 and 2).

Among the included studies, five studies (including 2608 eyes) reported data for GA groups stratified by classification 1, which classified GA lesions into CPI or CPS groups based on involvement of the center point of the macular. Three studies (including 386 eyes) reported data for GA groups stratified by classification 2, which classified GA lesions into FZI or FZS groups based on involvement of the foveal zone. Descriptive information for the eight studies is provided in Table 1. In studies that reported the baseline GA sizes in individual groups, the baseline GA sizes in the CPI (5.106 ± 0.124 mm^2) and CPS (4.677 ± 0.102 mm^2) groups are similar, and the baseline GA sizes in the FZI (8.348 ± 0.686 mm^2) and FZS (6.940 ± 0.712 mm^2) groups are comparable.

Four studies (including 480 eyes) reported the topographic distributions of GA lesions in at least two topographic zones at each follow-up. Descriptive information for the four studies is provided in Table 2.[4,5,9,17] Of note, one study (the geographic atrophy progression study)[13,17] reported data for GA groups stratified by classification 1 and data regarding topographic distributions of GA lesions in at least two topographic zones. Thus, this study was included in two separate analyses. The excluded articles and reasons for exclusion are listed in Supplementary Table S2. All 11 included articles were deemed to have a low risk of bias as assessed by the Newcastle-Ottawa Scale (scores between 6 and 8; Supplementary Table S3).

The Growth Rate of GA Involving the Center Point or Foveal Zone Is Lower

The forest plots showing the GA area growth rates (mm^2/year) in the four GA location groups (CPI, CPS, FZI, and FZS groups) are shown in Supplementary Figure S1. The forest plots comparing the GA area growth rate between the pair in classification 1 (CPI versus CPS) and the pair in classification 2 (FZI vs. FZS) are shown in Supplementary Figure S2. From the random-effects meta-analyses shown in the forest plots, the GA area growth rate was 33.1% higher in the CPS group (1.995 ± 0.261 mm^2/year) than in the CPI group (1.499 ± 0.180 mm^2/year) ($P < 0.001$) (Supplementary Fig. S3). Similarly, the GA area growth rate was found to be 58.8% higher in the FZS group (2.196 ± 0.130 mm^2/year) than in the CPI group (1.383 ± 0.094 mm^2/year) ($P < 0.001$) (Supplementary Fig. S3).

In our previous study as well as others, the GA area growth rate was found to be correlated with baseline lesion sizes, and the effective radius growth rate was less independent of the baseline lesion sizes.[21–23] Thus, to better account for different baseline lesion sizes, we determined the GA effective radius growth rate (mm/year) in all four GA location groups using random-effects meta-analyses (Supplementary Fig. S4). We then conducted random-effects meta-analyses to compare the effective radius growth rate between the CPI and CPS groups and between the FZI and FZS groups (Fig. 2). As demonstrated in Figures 2 and 3A, the GA effective radius growth rate was 30.1% higher in the CPS group (0.203 ± 0.013 mm/year) than in the CPI group (0.156 ± 0.011 mm/year) ($P < 0.001$); the GA effective radius growth rate was 61.7% higher in the FZS group (0.215 ± 0.012 mm/year) than in the FZI group (0.133 ± 0.009 mm/year) ($P < 0.001$). Interestingly, the mean difference in the GA effective radius growth rate between the pair in classification 2 (0.082 ± 0.014 mm/year between the FZS and FZI groups) was 70.8% higher than that in classification 1 (0.048 ± 0.005 mm/year between the CPS and CPI groups) ($P = 0.01$) (Fig. 3B). This result suggests that the involvement of the foveal zone (classification 2) is a more clinically significant prognostic factor to predict the GA growth rate compared to the involvement of the center point of the macula (classification 1).

Investigative Ophthalmology & Visual Science

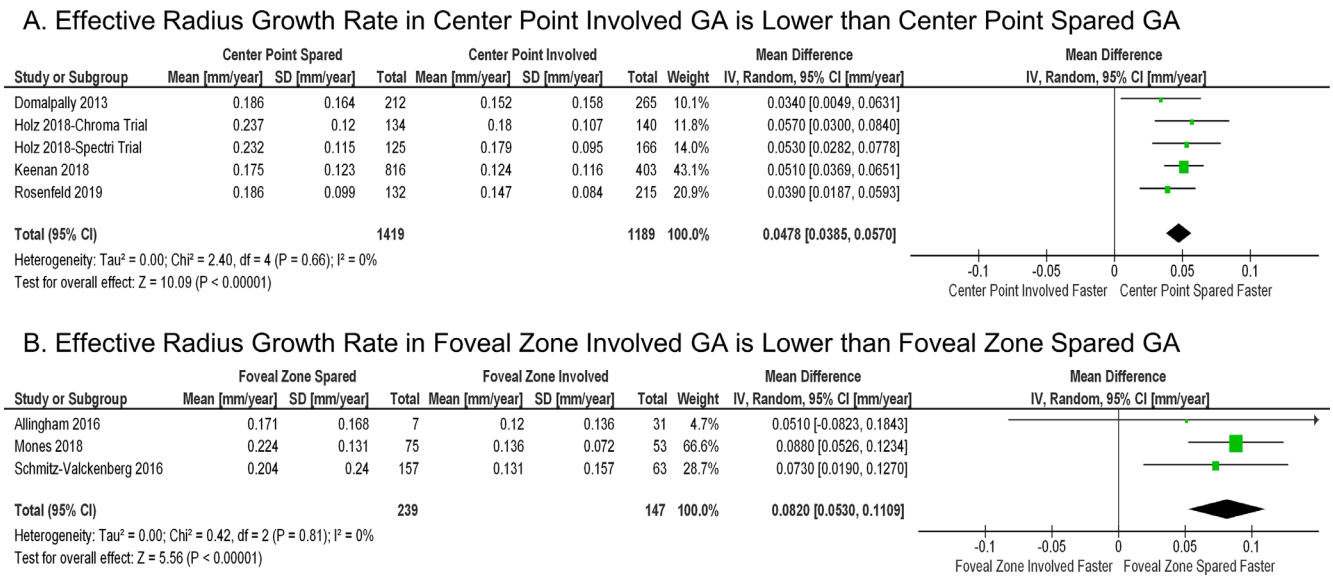

Figure 2. Random-effects meta-analysis comparing the effective radius growth rates (mm/year) of GA lesions with different lesion locations. **(A)** In GA location classification 1, the effective radius growth rate in the center point spared group is 0.048 mm/year faster than in the center point involved group ($P < 0.001$). **(B)** Similarly, in GA location classification 2, the effective radius growth rate in the foveal zone spared group is 0.082 mm/year faster than in the foveal zone involved group ($P < 0.001$). The diamond represents the overall effect estimate (width of the diamond represents the 95% CIs). For each individual study, different data marker sizes indicate weight, and the lines represent the 95% CIs. SD, standard deviation; CI, confidence interval.

To investigate the robustness of our results, we next analyzed the heterogeneity, sensitivity of the results, and confounding factors. We did not find any significant heterogeneity in the meta-analyses comparing the pairs in the two classifications; I^2 ranged from 0% to 32%, as shown in Figure 2 and Supplementary Figure S2. The sensitivity analysis shows that after removing one study at each time, the statistical significances in Figure 2 and Supplementary Figure S2 did not change significantly, suggesting that our results were not driven by any one of the included studies. In the stratified analysis, the GA effective radius growth rate was consistent between prospective interventional studies and prospective observational studies (0.179 $\pm$ 0.010 vs. 0.193 $\pm$ 0.014 mm/year; $P = 0.56$) (Supplementary Fig. S5). After the removal of one retrospective observational study, the GA growth rate in the FZS group was still significantly higher than the growth rate in the FZI group ($P < 0.001$), and the difference in the GA growth rate between the two groups was unaffected (Supplementary Fig. S6). Similarly, there was no significant difference in the GA growth rate reported by studies using fundus autofluorescence (0.186 $\pm$ 0.010 mm/year) versus studies using color fundus photography (0.178 $\pm$ 0.013 mm/year) ($P = 0.65$) (Supplementary Fig. S7). Also, the choice of imaging method did not affect the estimated difference in the GA growth rate between the CPS and CPI groups (Supplementary Fig. S8).

To examine the long-term natural history of GA lesions in each group (Fig. 4A), we introduced horizontal translation factors to correct for different initial GA sizes within each group. After the introduction of translation factors, the cumulative dataset of each group fit into a straight line with a very high value of r^2 (between 0.98 and 0.99) over nearly 10 years (Fig. 4B), suggesting that the GA effective radius increases linearly over the elapsed time in each GA group but with a distinct growth rate.

The GA Growth Rate Varies Across Topographic Zones in the Retina

Using the previously defined topographic zones and the reported GA growth rates in the zones from previous studies (Table 2), we estimated the mean GA effective radius growth rate in eight extrapolated topographic zones (Supplementary Table S4). Very interestingly, within the macula (0–3000 µm from the foveal center), the GA effective radius growth rate appeared to increase continuously as a function of the retinal eccentricity with a 3.2-fold difference between the maximum and minimum growth rate. The growth rate was then dramatically lower beyond the macular region (i.e., >3600 µm from the foveal center) (Fig. 5). Integration of the GA effective radius growth rate with the retinal eccentricity followed a sigmoidal curve (Supplementary Fig. S9A), suggesting that the topographic profile of the GA effective radius growth rate could fit a Gaussian function (Supplementary Fig. S9B). We then used this derived function to model the GA expansion over 30 years in different scenarios (Fig. 6). The modeling predicted that a GA lesion starting in the foveal center would grow symmetrically and remain as a circular shape (Fig. 6A and Supplementary Video S1). However, if two GA lesions started in the parafovea (retinal eccentricity of 1500 µm), they would first progress into individual small circular lesions; over time, the two lesions would grow into two kidney-shaped lesions, then merge into a single horseshoe-shaped lesion, and eventually cover the entire macula (Fig. 6B and Supplementary Video S2). Because the median number of GA lesions in patients has been reported to be three and the individual GA lesions usually do not have the same sizes (suggesting different onset times),[35] we modeled three GA lesions with different onset times (5 years apart) starting in the parafovea (Fig. 6C). Interestingly, the three GA lesions would grow into a ring-shaped lesion with fovea sparing and eventually cover the

Investigative Ophthalmology & Visual Science

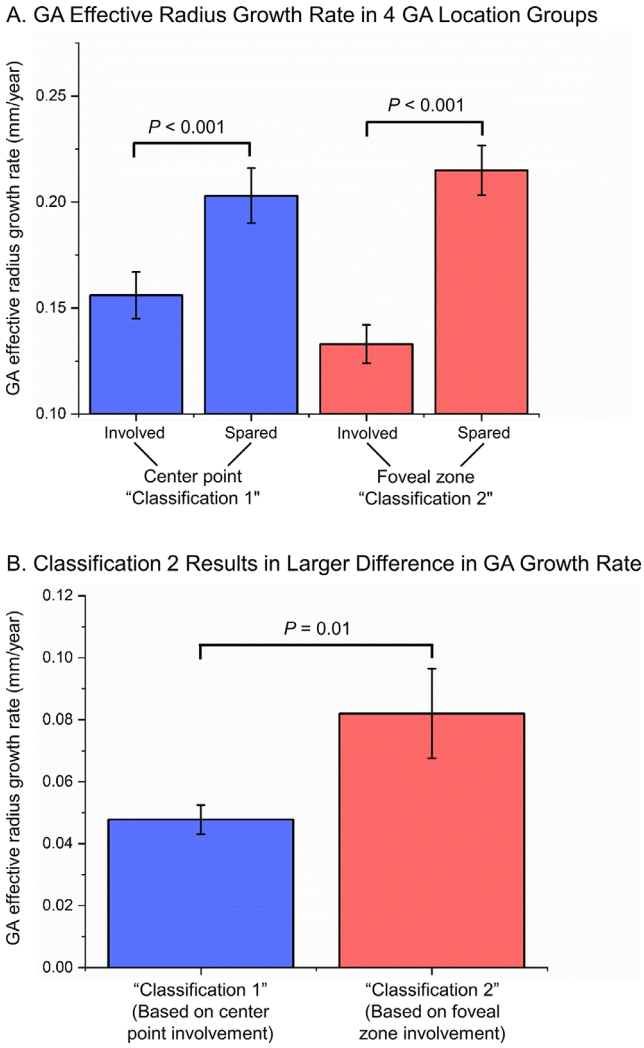

Figure 3. **(A)** GA effective radius growth rates (mm/year) in four GA location groups. The GA effective radius growth rate in each group was calculated from a random-effects meta-analysis shown in Supplementary Figure S4. The *P* values between the pair in classification 1 (i.e., classifying GA lesions based on center point involvement) and between the pair in classification 2 (i.e., classifying GA lesions based on foveal zone involvement) are from Figure 2 and are statistically significant. **(B)** The mean difference in the GA effective radius growth rate between the pair in classification 2 (0.082 ± 0.014 mm/year in red bar) is 70.8% larger than the mean difference between the pair in classification 1 (0.048 ± 0.005 mm/year in blue bar) ($P = 0.01$ from *t*-test). The error bar represents the standard error.

entire fovea (Fig. 6C and Supplementary Video S3), which is similar to the clinical observations of GA expansions starting outside the foveal island.[4,36]

Discussion

To the best of our knowledge, this is the first systematic review and meta-analysis to investigate the variation of GA growth rates across different topographic locations in the retina. The present meta-analysis estimated the effective radius growth rate (mm/year) of GA lesions in four location groups classified by two different schemes (i.e., center point involved or spared in classification 1 and foveal zone involved or spared in classification 2). We validated the ability of each classification to result in a statistically significant difference in the GA growth rate between two classified groups ($P < 0.001$). Interestingly, the clinical significance of the two classifications may not be equal. We found that the mean difference in the GA growth rate between the two groups in classification 2 (0.082 ± 0.014 mm/year) was 70.8% higher than that in classification 1 (0.048 ± 0.005 mm/year) ($P = 0.01$) (Fig. 3B). The current data suggest that, although classification 2 (three studies with 386 eyes) was less popular than classification 1 (five studies with 2608 eyes), the GA involvement of the foveal zone (i.e., classification 2) may be a stronger biomarker to predict the GA growth rate and allow stratification for confounding in clinical trials.

The current terminologies used to describe the location of GA lesions were highly inconsistent in the literature, with at least five different terminologies being reported: foveal or extrafoveal,[13,15,16] center involved or not involved,[10] central or noncentral,[12] subfoveal or non-subfoveal,[11] and with or without RPE atrophy under the foveal center.[14] To resolve the conflicts and avoid potential confusions, we propose the use of the terms "center point involved" or "center point spared" to describe GA involvement of the center point of the macula (i.e., classification 1), and we propose the use of the terms "foveal zone spared" and "foveal zone involved" to describe GA involvement of the foveal zone (i.e., classification 2), which can be defined as the central circular zone that is 750 µm in radius.[32]

A priori, there are at least two possible explanations for the observed association between the baseline location of GA lesions and the GA growth rate. First, it is possible that patients with GA involving the foveal zone represent a different patient population compared to patients with GA sparing the foveal zone and that each population has a distinct GA growth rate. However, a second compelling and more unifying hypothesis is that these patients all represent the same disease cohort but the GA progresses at different speeds across different topographic zones in the same retina. After gathering all data from the previous studies that assessed the GA growth rate in at least two different topographic zones in the retina, we estimated the GA effective radius growth rate in eight topographic zones (Supplementary Table S4 and Fig. 5). Interestingly, the GA growth rate in the outer zone of the macula (0.131 mm/year 1800–3000 µm from the foveal center) is 3.2-fold faster than the growth rate in the inner zone of the macula (0.041 mm/year 0–500 µm from the foveal center), which supports the second hypothesis. Moreover, the growth rate appeared to vary continuously as a function of the distance to the foveal center and fit a Gaussian-like function (Supplementary Fig. S9B). Note, we chose the Gaussian function to fit the topographic profile of the GA linear growth rate because of its simplicity. Future studies using individual-level data are needed to provide more data points for refining this topographic profile of GA growth rates.

Previous studies reported many GA configurations, including "small," "solid/unifocal" (including circular, oval, or kidney-shaped solitary lesions), "multifocal," "horseshoe," and "ring,"[5,37] but the underlying mechanism for the various configurations remains unknown. Our study suggests that the occurrence of different shapes of GA lesions may not be random. Rather, the different patterns that we observe may simply be due to the fact that the GA growth rate changes at different retinal locations, leading GA lesions to evolve into

Investigative Ophthalmology & Visual Science

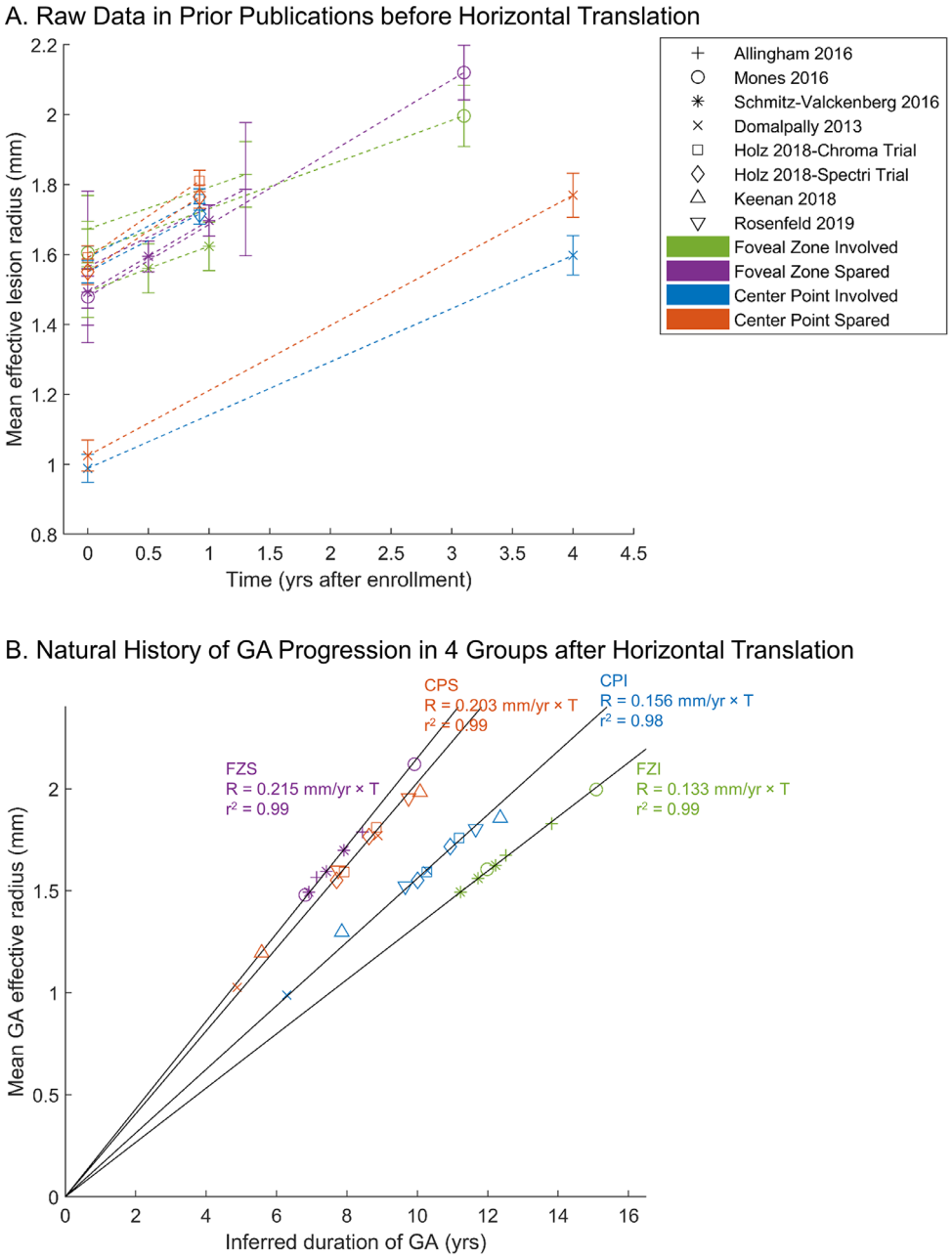

Figure 4. GA effective radius as a function of time in four GA location groups. The shape of the markers represents the corresponding study, and the color represents one of the four GA location groups. **(A)** Raw data in prior publications (error bars = standard errors). Note that the initial sizes of GA ranged from 0.99 mm to 1.67 mm in effective radius (3.07–8.79 mm^2 in area) among all studies, suggesting that these initial time points represent differing stages of disease. **(B)** After the introduction of translation factors (expressed in years in Table 1) to correct for different entry times of patients into each clinical study, cumulative datasets in each group fit along a straight line with a very high r^2, suggesting that the GA effective radius enlarges linearly over time in each GA location group. In the GA location classification 1, the GA growth rate in the CPS group (0.203 ± 0.013 mm/year) is 30.1% higher than that in the CPI group (0.156 ± 0.011 mm/year). In comparison, the GA growth rate in the FZS group (0.215 ± 0.012 mm/year) is 61.7% higher than the growth rate in the FZI group (0.133 ± 0.009 mm/year) using the GA location classification 2.

the various shapes at different time points. This hypothesis is also consistent with a previous observation that more than 50% of GA lesions changed from one configuration to another over a few years.[5] By applying our Gaussian topographic profile of the GA effective radius growth rate (Supplementary Fig. S9B), we were able to model the course of GA expansions over the elapsed time (Fig. 6). Importantly, our model gave rise to multiple GA shapes (circular/oval, kidney-shaped, horseshoe, and ring at different stages of GA; see Figs. 6B and 6C) that are consistent with the configurations reported in the literature. Also, we predicted that a GA lesion starting in the foveal center would remain symmetric and circular (Fig. 6A), and GA lesions starting in the parafovea would cover the majority of the macula over a long period of time while still sparing part of the fovea until late in the course of the disease (second to the bottom images

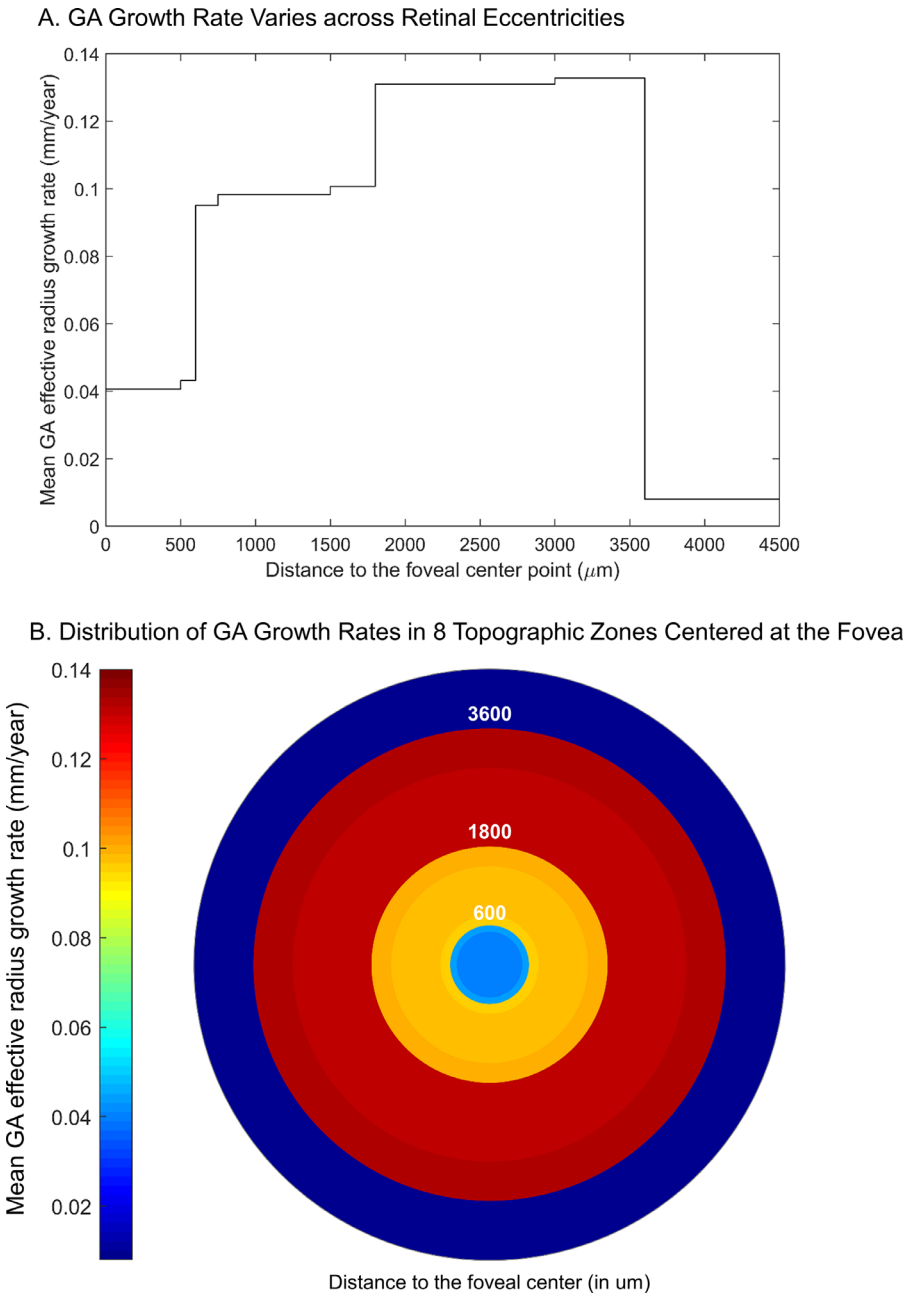

Figure 5. The GA effective radius growth rate varies across different topographic zones. **(A)** Using the previously reported GA growth rates in different retinal zones (Table 2), we estimated the weighted mean GA effective radius growth rates in eight topographic zones in the retina (numerical data shown in Supplementary Table S4) and plotted the growth rate as a function of retinal eccentricity (μm). Interestingly, the GA effective radius growth rate appears to increase continuously within the macula (i.e., from 0 to ~3000 μm from the foveal center) and then drops outside the macula. Note, there is a 3.2-fold difference between the maximum and minimum GA growth rate within the macula. **(B)** Heat map shows the variation of GA effective radius growth rate in eight topographic zones with different radii (μm) centered at the foveal center.

in both Figs. 6B and 6C, referred to by others as foveal sparing phenomenon). Both predictions corresponded well with previous observations.[5–7,38]

Although the underlying mechanisms for the differential growth rates in different topographic regions in the retina are unknown, several hypotheses have been proposed. For example, it was speculated that the high density of cones in the fovea are less susceptible to cell death compared to the rods system in the parafovea.[39–43] Some other groups suggested that the relatively increased choroidal blood supply might be protective to the fovea.[17,44,45] This may be supported by the findings that eyes with decreased choriocapillaris density are correlated with increased size and/or number of drusens,[46] and may also be supported by a recent study including an analysis of 33 eyes that found a positive correlation between the GA growth rate and the choriocapillaris flow impairment around the GA lesions.[47] The third hypothesis is based on the observation of the relatively high risk of developing AMD in eyes with decreased values of macular pigment.[48] In this hypothesis, the high density of

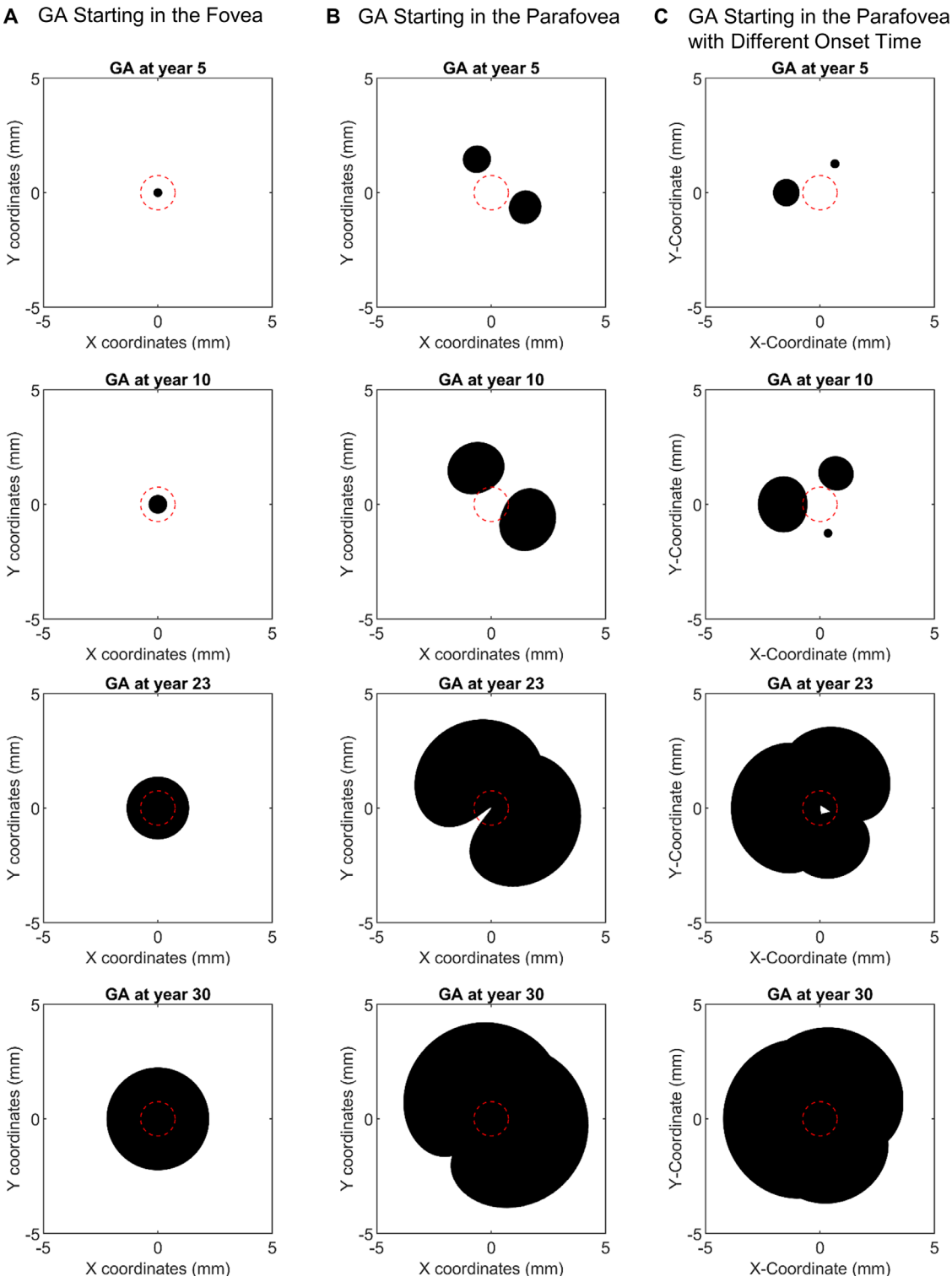

Figure 6. Images showing the modeling of GA expansion in three scenarios. The modeling is based on the Gaussian function between the GA effective radius growth rate and the distance to the foveal center shown in Supplementary Figure S9B. The origin of the coordinates represents the foveal center. The center red circle represents the foveal island with a radius of 0.75 mm. **(A)** GA lesions starting at the foveal center would grow symmetrically and remain as a circular shape over the elapsed time (from top to bottom images). **(B)** Two GA lesions starting in the parafovea (1.5 mm away from the foveal center) would first become small circular/oval lesions. Over the elapsed time, the two lesions would grow into kidney-shaped lesions, merge into a horseshoe-shaped lesion, and eventually cover the entire macula. **(C)** Three GA lesions with different onset times (5 years apart) starting in the parafovea would grow into a ring-shaped lesion with foveal sparing and eventually cover the entire fovea. The predicted shapes of GA lesions are similar to previously reported lesion shapes. Video clips showing continuous expansion of GA lesions in the 3 scenarios are provided in Supplementary Movies S1–S3.

Investigative Ophthalmology & Visual Science

macular pigment in the fovea may exhibit a protective effect and hinder GA progression. Although our findings might not exclude any of the hypotheses, the observed continuous variation of the GA growth rate across different retinal eccentricities points toward a local explanation (e.g., local anatomic variations) for the differential growth rates, rather than a systemic reason that would affect a topographic region homogeneously.

Quality of the Evidence and Study Limitations

This study constitutes a meta-analysis of 11 studies with 3254 unique eyes. The qualities of the included studies were high, with scores on the Newcastle-Ottawa Scale ranging between 6 and 8 (out of a possible 8). Due to the relatively small number of included studies for each random-effects meta-analysis (fewer than 10), we did not perform tests for funnel plot asymmetry to assess publication bias.[49] We found no significant interstudy heterogeneity among the included studies as assessed by the I^2 statistical test in the random-effects meta-analyses shown in Figure 2 and Supplementary Figure S2. The sensitivity analysis showed that no single study affected the statistical significance in the random-effects meta-analyses. The stratified analysis demonstrated that different imaging methods or study types did not significantly affect the main conclusions, which supports the validity of our present meta-analysis results.

This meta-analysis is not without its limitations. First, there are some limitations that are intrinsic to a meta-analysis. Because only the study-level data instead of the patient-level data are available for the present meta-analysis, we were limited to using summary data to estimate the growth rate of GA lesions with different topographic locations. Because of variations in the methodological designs, patient populations, and other factors across different studies, the associations found in the meta-analysis might have been confounded by these disparities. We used two approaches to address this issue. We addressed the limitation of the possible unexplained heterogeneity across studies by choosing a random effects approach in the meta-analysis to estimate and compare the GA growth rate in location groups (as suggested by the Cochrane Collaboration).[49] To further explore the impact of potential confounding factors, we performed subgroup analyses stratified by study designs and imaging methods. The results suggested that neither the study design nor the choice of imaging method affected the main conclusions significantly (Supplementary Figs. S5–S8). However, due to the limited number of studies in the literature that have investigated the association between the GA growth rate and topographic locations, we were unable to investigate the impact of other potential confounding factors (e.g., patient demographics, other characteristics of GA lesions).

Second, only four studies in the literature investigated the GA progression in at least two different topographic zones. The low number of studies might cause inaccuracy in the estimated GA effective radius growth rate in different zones, especially in regions outside of the macula, where only one study (Mauschitz et al.[17]) assessed the GA growth rate. Due to the limited number of studies, we were unable to perform a subgroup analysis to explore confounding effects. Thus, further longitudinal studies with a large number of patients affected by GA are needed to investigate the GA growth rate (mm/year) in linear axes in different retinal locations. Despite the limited data in the current literature, the modeling of GA expansion (Fig. 6) based on the derived topographic profile of the GA growth rate (Fig. 5) was consistent with the clinical observations of GA progression and resulted in various shapes of GA lesions described in the previous literature.[4,36] Third, in the literature, only three studies (386 eyes) used classification 2 to describe GA locations, as compared to the studies using classification 1 (five studies with 2608 eyes). To further compare the two classifications, a large longitudinal cohort study is needed to compare the effective radius growth rate of GA lesions in the spared and involved groups based on each classification.

Fourth, extrapolations necessary to determine the unreported values in some studies might have introduced biases into the outcomes. For example, Lindner et al.[4] did not specify an exact definition of the residual foveal island, so we used the reported average radius of the fovea (750 µm) as the cut-off radius for this zone.[32] As a comparison, we excluded this study and repeated all related analyses. We did not find any significant change in our results, and the topographic profile of the GA effective radius growth rate still fit a similar Gaussian function (Supplementary Fig. S9). Finally, because several of the studies we included were observational studies, survival bias is a potential concern.

In conclusion, this meta-analysis demonstrates that the topographic location is a significant prognostic factor for the GA growth rate. The classification of GA lesions into foveal zone involved and spared groups can result in a more significant difference in the GA growth rates between the two groups. The study also suggests that the GA progression speed varies continuously as a function of the retinal eccentricity, and there is a 3.2-fold difference between the maximum and minimum GA effective radius growth rate within the macula. This finding, combined with our modeling of GA expansion, may explain the various shapes of GA lesions and the foveal sparing phenomenon. These results may improve our understanding of the natural GA progression, especially across different retinal locations, and assist in the design of future clinical trials. However, future clinical and histological studies are required to generate a more refined topographic profile of the GA growth rate and determine the underlying biological mechanisms for the differential GA growth rate across the retina.

Acknowledgments

The authors thank Michael J. Allingham MD, PhD (Duke University Medical Center, Durham, NC) for sharing their data; Feimei Liu (Department of Biomedical Engineering, Yale University, New Haven, CT) for her help with the article screening; and Vermetha Polite and Khadija El-hazimy (Harvey Cushing/John Hay Whitney Medical Library, Yale University, New Haven, CT) for their technical assistance. This publication was made possible by the Yale School of Medicine Medical Student Research Fellowship.

Disclosure: **L.L. Shen**, None; **M. Sun**, None; **S. Khetpal**, None; **H.K. Grossetta Nardini**, None; **L.V. Del Priore**, Astellas Institute for Regenerative Medicine(C)

References

1. Blair CJ. Geographic atrophy of the retinal pigment epithelium: a manifestation of senile macular degeneration. *Arch Ophthalmol*. 1975;93:19–25.
2. Wong WL, Su X, Li X, et al. Global prevalence of age-related macular degeneration and disease burden projection

for 2020 and 2040: a systematic review and meta-analysis. *Lancet Glob Health*. 2014;2:e106–e116.
3. Fleckenstein M, Mitchell P, Freund KB, et al. The progression of geographic atrophy secondary to age-related macular degeneration. *Ophthalmology*. 2018;125:369–390.
4. Lindner M, Boker A, Mauschitz MM, et al. Directional kinetics of geographic atrophy progression in age-related macular degeneration with foveal sparing. *Ophthalmology*. 2015;122:1356–1365.
5. Sunness JS, Gonzalez-Baron J, Applegate CA, et al. Enlargement of atrophy and visual acuity loss in the geographic atrophy form of age-related macular degeneration. *Ophthalmology*. 1999;106:1768–1779.
6. Sunness JS, Rubin GS, Zuckerbrod A, Applegate CA. Foveal-sparing scotomas in advanced dry age-related macular degeneration. *J Vis Impair Blind*. 2008;102:600–610.
7. Schmitz-Valckenberg S, Fleckenstein M, Helb HM, Charbel Issa P, Scholl HP, Holz FG. In vivo imaging of foveal sparing in geographic atrophy secondary to age-related macular degeneration. *Invest Ophthalmol Vis Sci*. 2009;50:3915–3921.
8. Mones J, Biarnes M, Trindade F, Arias L, Alonso J. Optical coherence tomography assessment of apparent foveal swelling in patients with foveal sparing secondary to geographic atrophy. *Ophthalmology*. 2013;120:829–836.
9. Sayegh RG, Sacu S, Dunavölgyi R, et al. Geographic atrophy and foveal-sparing changes related to visual acuity in patients with dry age-related macular degeneration over time. *Am J Ophthalmol*. 2017;179:118–128.
10. Domalpally A, Danis RP, White J, et al. Circularity index as a risk factor for progression of geographic atrophy. *Ophthalmology*. 2013;120:2666–2671.
11. Holz FG, Sadda SR, Busbee B, et al. Efficacy and safety of lampalizumab for geographic atrophy due to age-related macular degeneration: Chroma and Spectri phase 3 randomized clinical trials. *JAMA Ophthalmol*. 2018;136:666–677.
12. Keenan TD, Agron E, Domalpally A, et al. Progression of geographic atrophy in age-related macular degeneration: AREDS2 Report Number 16. *Ophthalmology*. 2018;125:1913–1928.
13. Schmitz-Valckenberg S, Sahel JA, Danis R, et al. Natural history of geographic atrophy progression secondary to age-related macular degeneration (Geographic Atrophy Progression Study). *Ophthalmology*. 2016;123:361–368.
14. Rosenfeld PJ, Dugel PU, Holz FG, et al. Emixustat hydrochloride for geographic atrophy secondary to age-related macular degeneration: a randomized clinical trial. *Ophthalmology*. 2018;125:1556–1567.
15. Monés J, Biarnes M. The rate of progression of geographic atrophy decreases with increasing baseline lesion size even after the square root transformation. *Transl Vis Sci Technol*. 2018;7:40.
16. Allingham MJ, Nie Q, Lad EM, et al. Semiautomatic segmentation of rim area focal hyperautofluorescence predicts progression of geographic atrophy due to dry age-related macular degeneration. *Invest Ophthalmol Vis Sci*. 2016;57:2283–2289.
17. Mauschitz MM, Fonseca S, Chang P, et al. Topography of geographic atrophy in age-related macular degeneration. *Invest Ophthalmol Vis Sci*. 2012;53:4932–4939.
18. Stroup DF, Berlin JA, Morton SC, et al. Meta-analysis of observational studies in epidemiology: a proposal for reporting. *JAMA*. 2000;283:2008–2012.
19. Lindblad AS, Lloyd PC, Clemons TE, et al. Change in area of geographic atrophy in the age-related eye disease study: AREDS Report Number 26. *Arch Ophthalmol* 2009;127:1168–1174.
20. Krishnadev N, Meleth AD, Chew EY. Nutritional supplements for age-related macular degeneration. *Curr Opin Ophthalmol*. 2010;21:184.
21. Shen L, Liu F, Grossetta Nardini H, Del Priore LV. Natural history of geographic atrophy in untreated eyes with nonexudative age-related macular degeneration: a systematic review and meta-analysis. *Ophthalmol Retina*. 2018;2:914–921.
22. Yehoshua Z, Rosenfeld PJ, Gregori G, et al. Progression of geographic atrophy in age-related macular degeneration imaged with spectral domain optical coherence tomography. *Ophthalmology*. 2011;118:679–686.
23. Feuer WJ, Yehoshua Z, Gregori G, et al. Square root transformation of geographic atrophy area measurements to eliminate dependence of growth rates on baseline lesion measurements: a reanalysis of age-related eye disease study report no. 26. *JAMA Ophthalmol*. 2013;131:110–111.
24. Viechtbauer W. Conducting meta-analyses in R with the metafor package. *J Stat Softw*. 2010;36:1–48.
25. Riley RD, Moons KGM, Snell KIE, et al. A guide to systematic review and meta-analysis of prognostic factor studies. *BMJ*. 2019;364:k4597.
26. Liu TYA, Shah AR, Del Priore LV. Progression of lesion size in untreated eyes with exudative age-related macular degeneration: a meta-analysis using Lineweaver-Burk plots. *JAMA Ophthalmol*. 2013;131:335–340.
27. Shah AR, Del Priore LV. Natural history of predominantly classic, minimally classic, and occult subgroups in exudative age-related macular degeneration. *Ophthalmology*. 2009;116:1901–1907.
28. Shah AR, Del Priore LV. Progressive visual loss in subfoveal exudation in age-related macular degeneration: a meta-analysis using Lineweaver-Burke plots. *Am J Ophthalmol*. 2007;143:83–89.e82.
29. Shen LL, Liu F, Nardini HG, Del Priore LV. Reclassification of fundus autofluorescence patterns surrounding geographic atrophy based on progression rate: a systematic review and meta-analysis. *Retina*. 2019;39:1829–1839.
30. Shen LL, Liu F, Grossetta Nardini HK, Del Priore LV. Fellow eye status is a biomarker for the progression rate of geographic atrophy: a systematic review and meta-analysis. *Ophthalmol Retina*. 2019;3:305–315.
31. Shen LL, Sun M, Grossetta Nardini HK, Del Priore LV. Natural history of autosomal recessive Stargardt disease in untreated eyes: a systematic review and meta-analysis of study- and individual-level data. *Ophthalmology*. 2019;126:1288–1296.
32. Gass JDM. *Stereoscopic Atlas of Macular Diseases: Diagnosis and Treatment*. St. Louis, MO: Mosby-YearBook; 1987:464–469.
33. Wells G, Shea B, O'Connell D, et al. *The Newcastle-Ottawa Scale (NOS) for Assessing the Quality of Nonrandomised Studies in Meta-Analyses*. Ottawa, Ontario: Ottawa Health Research Institute, University of Ottawa; 2011. Available at: http://www.ohri.ca/programs/clinical_epidemiology/oxford.htm. Accessed June 11, 2017.
34. Luchini C, Stubbs B, Solmi M, Veronese N. Assessing the quality of studies in meta-analyses: advantages and limitations of the Newcastle Ottawa Scale. *World J Meta-Anal*. 2017;5:80–84.
35. Bellmann C, Jorzik J, Spital G, Unnebrink K, Pauleikhoff D, Holz FG. Symmetry of bilateral lesions in geographic atrophy in patients with age-related macular degeneration. *Arch Ophthalmol*. 2002;120:579–584.
36. Sarks JP, Sarks SH, Killingsworth MC. Evolution of geographic atrophy of the retinal pigment epithelium. *Eye*. 1988;2:552–577.
37. Holz FG, Bellman C, Staudt S, Schutt F, Volcker HE. Fundus autofluorescence and development of geographic atrophy

Investigative Ophthalmology & Visual Science

in age-related macular degeneration. *Invest Ophthalmol Vis Sci*. 2001;42:1051–1056.

38. Lindner M, Lambertus S, Mauschitz MM, et al. Differential disease progression in atrophic age-related macular degeneration and late-onset Stargardt disease. *Invest Ophthalmol Vis Sci*. 2017;58:1001–1007.
39. Chen C, Wu L, Wu D, et al. The local cone and rod system function in early age-related macular degeneration. *Doc Ophthalmol*. 2004;109:1–8.
40. Owsley C, Jackson GR, Cideciyan AV, et al. Psychophysical evidence for rod vulnerability in age-related macular degeneration. *Invest Ophthalmol Vis Sci*. 2000;41:267–273.
41. Wang J-S, Kefalov VJ. The cone-specific visual cycle. *Prog Retin Eye Res*. 2011;30:115–128.
42. Curcio CA, Medeiros NE, Millican CL. Photoreceptor loss in age-related macular degeneration. *Invest Ophthalmol Vis Sci*. 1996;37:1236–1249.
43. Owsley C, McGwin G, Jackson GR, Kallies K, Clark M. Cone-and rod-mediated dark adaptation impairment in age-related maculopathy. *Ophthalmology*. 2007;114:1728–1735.
44. Chuang E, Sharp D, Fitzke F, Kemp C, Holden A, Bird A. Retinal dysfunction in central serous retinopathy. *Eye*. 1987;1:120–125.
45. Xu W, Grunwald JE, Metelitsina TI, et al. Association of risk factors for choroidal neovascularization in age-related macular degeneration with decreased foveolar choroidal circulation. *Am J Ophthalmol*. 2010;150:40–47.e2.
46. Mullins RF, Johnson MN, Faidley EA, Skeie JM, Huang J. Choriocapillaris vascular dropout related to density of drusen in human eyes with early age-related macular degeneration. *Invest Ophthalmol Vis Sci*. 2011;52:1606–1612.
47. Nassisi M, Baghdasaryan E, Borrelli E, Ip M, Sadda SR. Choriocapillaris flow impairment surrounding geographic atrophy correlates with disease progression. *PLoS ONE*. 2019;14:e0212563.
48. Beatty S, Murray IJ, Henson DB, Carden D, Koh H-H, Boulton ME. Macular pigment and risk for age-related macular degeneration in subjects from a Northern European population. *Invest Ophthalmol Vis Sci*. 2001;42:439–446.
49. Higgins J, Green S, eds. *Cochrane Handbook for Systematic Reviews of Interventions*. Version 5.1.0 [updated March 2011]. London, UK: The Cochrane Collaboration; 2011.